AD-A104 505 MCDONNELL DOUGLAS ASTRONAUTICS CO-ST LOUIS MO F/G 16/4
UNCONSTRAINED SUPERSONIC CRUISE AND MANEUVERING CONFIGURATION C--ETC(U)
1979 R KRIEGER, J E GREGOIRE, R F HOOD F33615-77-C-3037
UNCLASSIFIED NL

END
DATE FILMED
0 81
DTIC

79-0220

Unconstrained Supersonic Cruise and Maneuvering Configuration Concepts

R.J. Krieger, J.E. Gregoire and R.F. Hood,
McDonnell Douglas Astronautics Co., St. Louis, Mo.

17th AEROSPACE SCIENCES MEETING

New Orleans, La./January 15-17, 1979

UNCONSTRAINED SUPERSONIC CRUISE AND MANEUVERING CONFIGURATION CONCEPTS

Robert J. Krieger*
with Joseph E. Gregoire and Richard F. Hood
McDonnell Douglas Astronautics Company, St. Louis, Mo.

Abstract

Configuration concepts are presented which have high lift-to-drag ratios and maneuverability achievable by relieving constraints due to carriage, propulsion and subsystem integration. Noncircular body, lifting body, blended wing-body, wing-body and favorable interference concepts are developed using aerodynamic design criteria derived for climb-cruise-intercept missions. The Hypersonic Arbitrary Body Program (HABP) is evaluated for predicting aerodynamic characteristics. Comparisons of wind tunnel data and predictions are presented. Major features such as a spatular nose, flat bottom, high fineness ratio, ramped nose, planar shape, high wing, end plated wing, and interference channel are shown to enhance aerodynamic characteristics.

Background

The configuration concepts described and analyzed in this paper were developed and tested as part of Phase I of the Aerodynamic Configured Missile (ACM) Development Program[1] funded by the Air Force Flight Dynamics Laboratory. ACM is a three phase program with an objective to provide innovative aerodynamic configuration concepts which significantly improve performance compared to present missile systems. In Phase I, unconstrained missile configuration concepts were investigated. The second and third phases of the program will reconfigure the best concepts selected in Phase I by applying the constraints which typically compromise the aerodynamic configuration of a missile, i.e., propulsion, carriage, cost, guidance, warhead and control. The configurations will be tailored to retain the Phase I aerodynamic characteristics to the greatest extent possible in the presence of constraints.

Nomenclature

α	=	angle of attack, referenced to the body centerline, degrees
β	=	angle of sideslip, referenced to the body centerline, degrees
ϕ	=	model roll angle (zero is upright), degrees
q	=	wind tunnel dynamic pressure
C_L	=	lift coefficient, lift/qS
C_D	=	drag coefficient, drag/qS
C_M	=	pitching moment coefficient, moment/qS
S	=	reference area (planform area)
L	=	reference length (model length)
C_p	=	pressure coefficient, Δ p/q
X_{CP}	=	longitudinal center of pressure
V	=	configuration volume

Subscripts:

opt	=	condition at which lift-over-drag is a maximum
man	=	maneuvering point (10g)
W	=	wave pressure (drag)
min	=	minimum (drag)

Development of Concepts

Ground Rules

Configurations were developed to satisfy two benchmark missions; long range air-to-ground cruise and long range air-to-air intercept. The long range cruise benchmark configuration had a mid-cruise weight of 1800 lbs. and a volume of 32 ft.^{3} The maneuvering benchmark configuration had a mid-cruise weight of 325 lbs. and a volume of 7.1 ft.^{3} Both had cruise lift-over-drag ratios of three. Since a high fineness ratio has a dramatic positive effect on lift-over-drag and since missile configurations (and wind tunnel models) must be diameter limited, a maximum fineness ratio of 15 was fixed as a development limit based on studies of structural limitations of current missile designs. In order to provide a variety in adaptability of constraints and to assure evaluation of a large number of diverse configurations, concepts were divided into five classes; noncircular body, lifting body, favorable interference, wing-body and blended wing-body. Body dominated shapes were emphasized because the body of a missile must provide much of the lift to carry its own weight at supersonic cruise conditions. This is because of the high density packaging of missile volume. Concepts would be developed into wind tunnel configurations that would 1) be "real" configurations, that is, would be sized to the volumes of the benchmark configurations, 2) have attractive features that can guide Phase II reconfiguring and 3) have shapes that fill data analysis gaps.

Literature Search

A literature search was performed to obtain as much experimental data as possible for configurations and test conditions that were consistent with the benchmark missions. The data was divided into the respective body and mission categories. The data base was examined for analysis gaps, areas where a lack of data was apparent or where analysis methods were not available. From this data base, promising aerodynamic features were identified, such as flat bottom, arrow and M wings, convex body splining and wave cancellation.

Development Techniques

Sensitivity studies were performed on the benchmark mission trajectories to identify aerodynamic characteristics that have first order effects on performance parameters. Point of departure configurations were selected from the data base for each concept class. These were configurations that exhibited the most desirable aerodynamic characteristics and yet had sufficient experimental data available. The aerodynamic characteristics of these configurations were then calculated, compared with the experimental data and, if necessary, appropriate adjustments made to pressure methods to achieve good comparisons. The primary prediction program employed was the Hypersonic Arbitrary Body Program (HABP)[2] which

was developed at McDonnell Douglas Corporation under contract to AFFDL. During this calibration process, one data gap that was identified was leeward side pressure measurements. Once confidence was established in our prediction of aerodynamic characteristics, changes could be made to the point of departure configurations using the list of attractive aerodynamic features. An example of this development technique is shown on Figure 1. The flat bottom ellipse configuration was the point of departure in the noncircular body class. Two aerodynamic features that provided dramatic improvement of aerodynamic characteristics were the nose ramp angle and the spatular nose. This improvement was achieved by reducing the nose impact angles at zero degree angle of attack, thereby reducing the point of minimum drag to zero angle of attack and consequently lowering α_{opt}. Features that produced these trends in the noncircular body class invariably increased lift-over-drag ratio. During the configuration development attention was also concentrated on volumetric efficiency, i.e., shapes that are rectangular or elliptic that promise easier constraint adaptability.

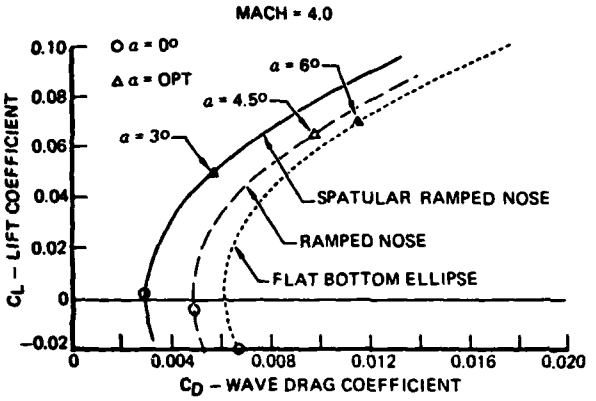

FIGURE 1 DEVELOPMENT OF SPATULAR NOSE

Wind Tunnel Configurations

The concepts developed and tested in the wind tunnel program are shown in Fig. 2 through 5. The noncircular body class shown in Fig. 2 consists of a real, volume sized configuration, B_2 N_2, as well as a planar shape, B_1 N_1. Primary B_2 N_2 features are the spatular nose, flat bottom, nose ramp angle and elliptic cross section. Additional features include blunt nose (N_4), rounded nose (N_5), increased ramp angle (N_3) and large (F_2) and small (F_1) fins mounted in vertical, ventral and canard type positions.

The lifting body configuration (B_3 N_8) is shown in Fig. 3. It includes a flat bottom, ramped nose, a boattail and is sized to benchmark volume. The triangular, planar nose (N_6) and spatular, elliptic nose (N_7) were designed to provide a drag tradeoff between a volumetrically efficient shape and a conventional pointed nose. The favorable interference concept, B_8, (shown here at reduced scale) is a two dimensional channel designed to cancel wave drag and produce high lift (through high compression pressures).

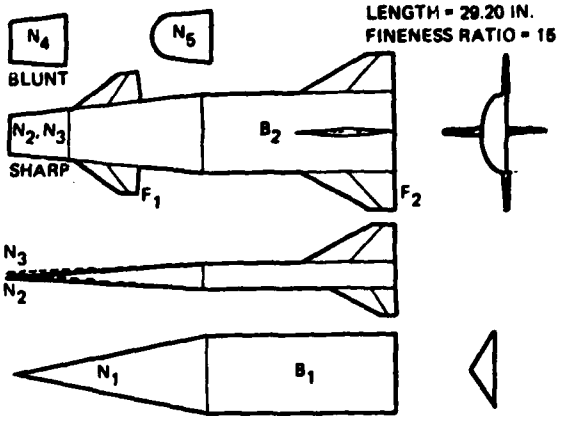

FIGURE 2 NON-CIRCULAR BODY CONCEPTS

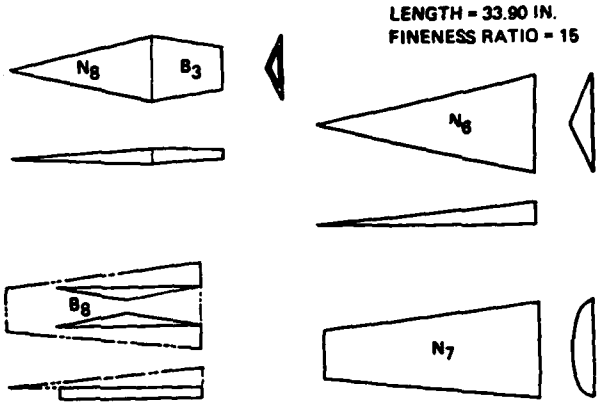

FIGURE 3 LIFTING BODY AND FAVORABLE INTERFERENCE CONCEPTS

The wing-body class concepts are shown in Fig. 4. The volume-sized configuration is B_5 W_1 which features an arrow wing, flat ramped nose and rectangular cross-section. Additional wing shapes developed include a delta, forward delta, clipped and M shape. The W_1 wing was also tested at incidence and with end plates designed to create wave riding flow on the wing.

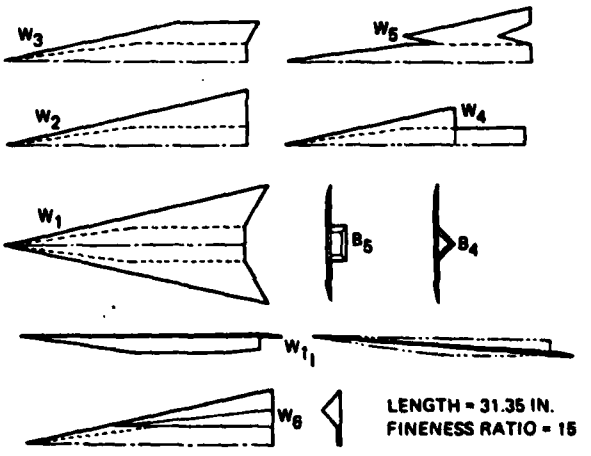

FIGURE 4 WING-BODY CONCEPTS

The blended wing-body concepts developed are shown in Fig. 5. Two shapes were investigated, a concave (real volume) and a convex blending shape. The configurations include a flat ramped nose and boattail and were tested with the W_1 arrow wing.

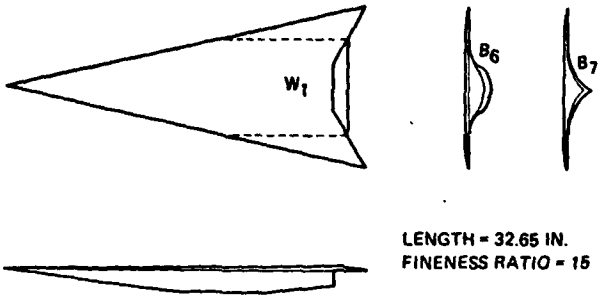

FIGURE 5 BLENDED WING-BODY CONCEPTS

Test Conditions

The ACM concepts were tested in the AEDC Von Karman Facility (VKF) Tunnel A (237 runs) and the AEDC Propulsion Wind Tunnel (PWT) four feet transonic wind tunnels (127 runs). The test program scope is shown in Fig. 6. Six-component force and moment data were obtained in both wind tunnels. All coefficients were referenced to planform area. All model base areas were corrected to freestream pressure. Moments were referenced to model length and reduced about 50% of length for all configurations. Reynolds number in the PWT was nominally 2 X 10^6/ft. Reynolds number in the VKF was approximately 2 X 10^6/ft. at low dynamic pressure conditions and 5-6 X 10^6/ft. at high pressure conditions. The pressure runs performed on the VKF consisted of leeward side measurements on the noncircular body (B_2 N_2) and lifting body (B_3 N_8) configurations and internal channel measurements on the favorable interference model (N_7 B_8). Schlieren photographs were obtained for all runs and oil flow photographs for selected configurations in the VKF. Configurations were tested upright and inverted in the VKF but upright only in the PWT. Bodies were tested with and without fins and wings. Configurations were tested up to 25 deg. angle of attack at zero yaw and 10 deg. yaw at zero angle of attack.

Test Results

Comparison With Predictions

The geometries of all configurations were modeled in HABP and aerodynamic characteristics were generated. Different pressure methods were used however in the various classes depending on the results experienced matching the aerodynamics of the point of departure configurations. The HABP pressure methods used are shown on Fig. 7 and are described in the HABP Users Manual[2]. Generally speaking, the test data agreed quite well with the predictions. Although maximum lift-over-drag ratios were slightly lower than predicted for most concepts, the relative ranking of one concept with respect to another was not altered by the wind tunnel results.

An example comparison is the Mach 4.0 blended wing body results shown in Fig. 8. The HABP predictions are compared with test data from both upright and inverted runs and show good agreement at C_{DMIN} and at $(L/D)_{MAX}$ of the upright run but poorer agreement for the inverted run. The poorer agreement in the inverted position is

VKF – TUNNEL A

CLASS	NO. OF CONFIG.	NO. OF RUNS	MACH					TYPE OF RUNS						
								PRESS	F&M				UP SIDE DOWN	OIL FLOW
									α-CUT		β-CUT			
			3.0	4.0	4.5	5.0	5.5		Hi_q	LO_q	Hi_q	LO_q	LO_q	
NON-CIRCULAR	9	74	22	25	0	27	0	9	9	21	7	12	13	3
LIFTING BODY	3	33	8	8	3	11	3	9	2	7	2	8	3	2
FAVORABLE INTERFERENCE	1	15	0	0	4	7	4	6	0	4	0	3	0	2
WING-BODY	10	77	24	27	0	26	0	0	3	30	1	20	18	5
BLENDED WING-BODY	4	38	12	14	0	12	0	0	0	12	0	12	12	2
TOTALS:	27	237	66	74	7	83	7	24	14	74	10	55	46	14

PWT–4T

CLASS	CONFIGURATIONS	NO. OF RUNS	MACH					TYPE OF RUNS	
			.55	.80	.95	1.1	1.2	α–CUT	β – CUT
NON-CIRCULAR	6	36	10	10	4	8	4	20	16
LIFTING BODY	1	8	2	2	2	2	0	4	4
WING-BODY	8	51	16	16	9	10	0	26	25
BLENDED WING-BODY	4	32	8	8	8	8	0	16	16
TOTALS	19	127	36	36	23	28	4	66	61

FIGURE 6 TEST PROGRAM SUMMARY

CONFIGURATION CLASS	WINDWARD	LEEWARD
NON-CIRCULAR	DAHLEM BUCK	DAHLEM-BUCK WITH CORRECTION APPLIED VERSUS ANGLE OF ATTACK
LIFTING-BODY	TANGENT WEDGE EMPIRICAL	VAN DYKE UNIFIED
WING-BODY AND BLENDED WING-BODY	TANGENT WEDGE USING OBLIQUE SHOCK	PRANDTL-MEYER

FIGURE 7 HABP PRESSURE METHODS

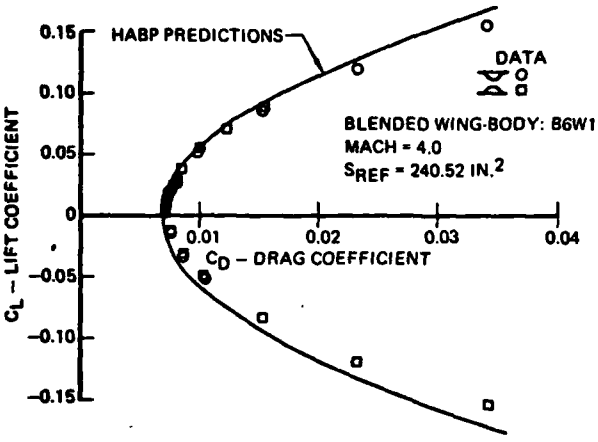

FIGURE 8 BLENDED BODY HABP COMPARISONS

attributed to the tangent wedge over prediction of flat bottom pressures. Noncircular body drag polar comparisons are shown in Fig. 9. Although there was excellent agreement at C_{DMIN}, $(L/D)_{MAX}$ was lower than predicted for both ellipse orientations. Lift and stability comparisons are shown in Fig. 10. The lift agreement at angle of attack with the flat bottom is excellent but the lift is over predicted with the elliptic side downward. The stability plot in this same figure show that this spatular nose configuration had a center of pressure forward of predictions. HABP had predicted neutral stability at α_{opt} but data showed the center of pressure was actually at 41% of length (flat bottom) and 45.5% (elliptic bottom). These differences were attributed to leeward side pressure distributions different than the predic-

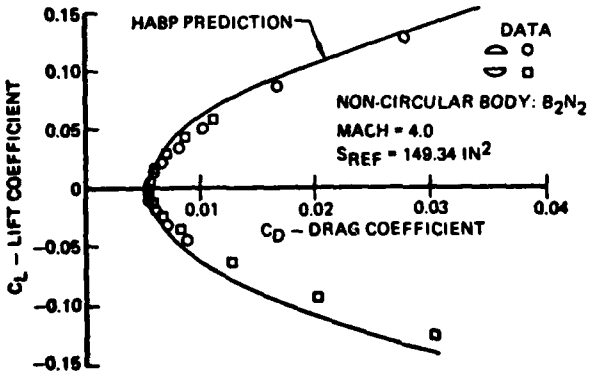

FIGURE 9 NON-CIRCULAR BODY HABP COMPARISONS

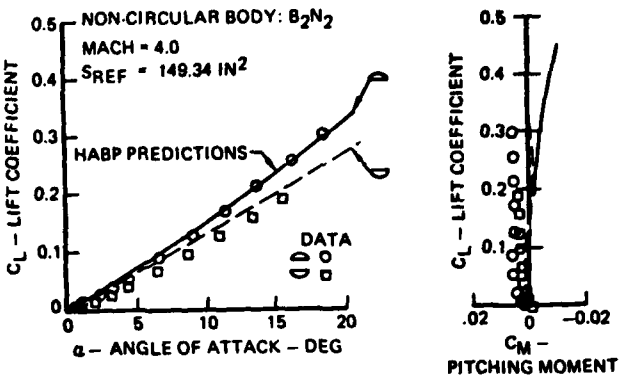

FIGURE 10 LIFT AND STABILITY HABP COMPARISONS

tions. Leeward side pressure measurements were made in anticipation of this problem. The data shown in Fig. 11 are an example of the results obtained. Variation with angle of attack agreed fairly well with predictions up to 10 deg. angle of attack but the pressure variation peripherally around the body was greater than predicted. Pressures at high angle of attack were consistently greater than $1/M^2$.

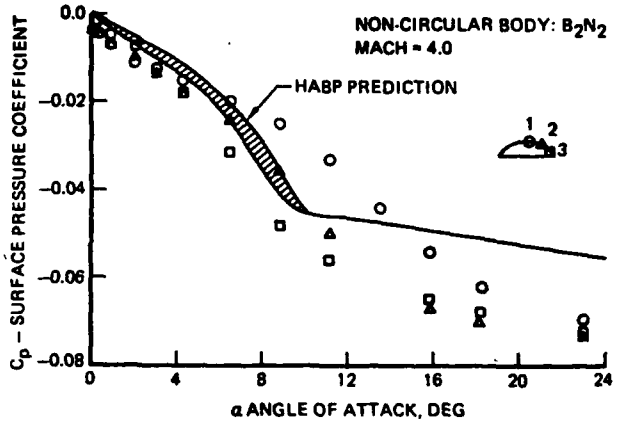

FIGURE 11 LEEWARD SIDE PRESSURES

Cruise Mission

Because the prediction techniques were more than adequate, the test results of the supersonic cruise concepts showed good aerodynamic potential. Lift-over-drag ratios from 5 to 7.5 were achieved, these were more than twice the benchmark configurations. The literature data base had shown the importance of planform in designing for high lift-over-drag ratios. This strong relationship is shown in Figs. 12 and 13. In Fig. 12 $(L/D)_{MAX}$ is plotted against the volume-to-planform ratio for the body-alone configuration. The data symbols indicate both cross section shape and orientation. In all cases, the flat bottom orientation achieved the higher $(L/D)_{MAX}$. Of these configurations only B_3 N_8 and B_2 N_2 are "real" configurations exhibiting volumetric efficiency. The highest $(L/D)_{MAX}$ is achieved by B_7. However, this convex blending concept also has the lowest potential for satisfying constraints.

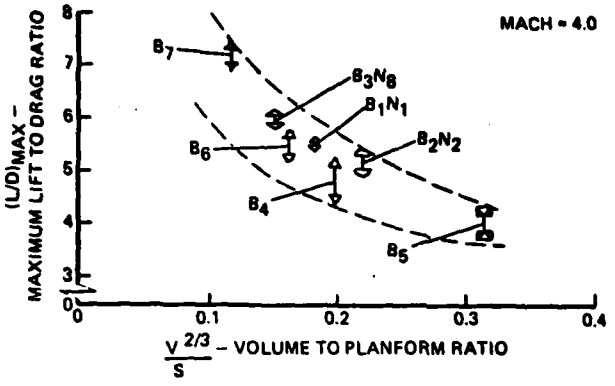

FIGURE 12 BODY L/D CHARACTERISTICS

The planform/volume relationship with $(L/D)_{MAX}$ is shown for winged configurations in Fig. 13. An interesting result is that the optimum orientation is flat top. The carryover flow of the body on the wing acts to increase lift at angles of attack near α_{opt}. The magnitudes of the carryover effect for the various body shapes is shown in the table of Fig. 14. The ΔC_L at zero angle of attack is a measure of the carryover flow because the wing is at zero incidence angle. Lift increments as large as 6.8% of $\Delta C_L/C_{L_{opt}}$ are achieved with the triangular body shape.

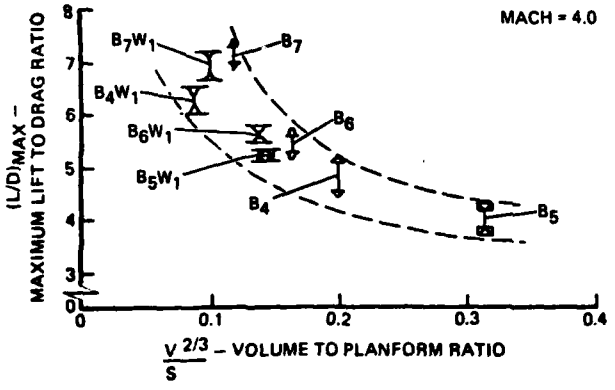

FIGURE 13 WING-BODY L/D CHARACTERISTICS

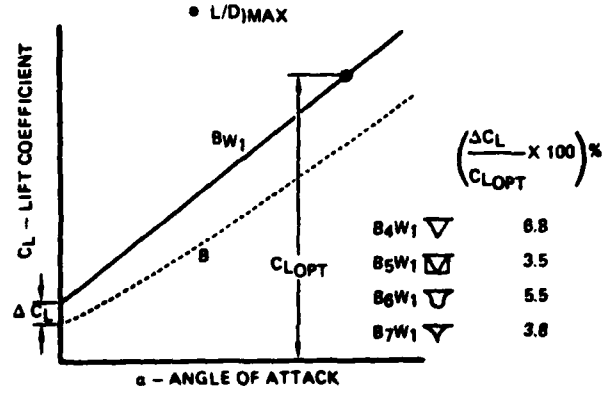

FIGURE 14 CARRYOVER FLOW EFFECTS

Other results include:

- The effect of the incidence wing was to merely shift α_{opt} with little change in $(L/D)_{MAX}$
- Of the wings on the shape parametric, the M-wing showed the most promise having the highest lift per exposed area
- The favorable interference configuration created high lift but boundary layer separation prevented the wave drag cancellation desired
- The increased ramp angle on B_2 N_2 provided a change in stability with little change on $(L/D)_{MAX}$
- The triangular, planar nose and spatular elliptic nose showed almost identical $C_{D_{MIN}}$ values

Maneuvering Mission

The configurations were scaled to the benchmark maneuvering mission volume, 7.1 $ft.^3$, and analyzed at their maneuvering altitude, (90K ft.) and load factor requirement (10g). The resulting direct relationship between planform area and lift-over-drag ratio is shown in Fig. 15. Although aerodynamic configuring has less effect on the maneuvering mission than in the cruise, the positive effect of flat bottom is readily apparent. All configurations have higher L/D ratios at their maneuvering point with flat bottom including the wing-bodies.

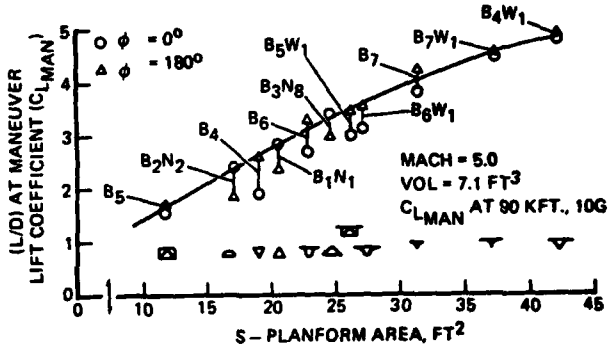

FIGURE 15 MANEUVER L/D CHARACTERISTICS

The flat bottom effect on lift-curve slope is shown in Fig. 16. The body configurations with either elliptic or triangular side down and the winged configurations with flat top have rather linear lift curves but all configurations with the flat bottom show greater second-order lift effects.

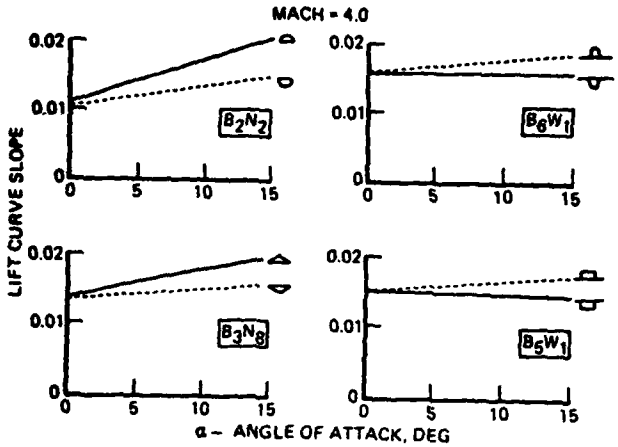

FIGURE 16 FLAT BOTTOM LIFT

Stability

One of the most common aerodynamic problems with air breathing supersonic missiles is stability. Many configurations tend to be unstable in boost (becuase of inlet covers) and too stable in sustain (causing high trim drag). The transonic PWT test was performed primarily to obtain stability data on our configurations over the entire mission Mach envelope. An example of the results is shown in Fig. 17 for a body configuration (B_2 N_2) and a winged configuration (B_6 W_1). These results are typical. The W_1 wing, has a centroid of area at 67% of length and has an aft c.p. throughout the mach range. The spatular nose and ramp angle on B_2 N_2 has a far forward c.p. throughout the Mach range.

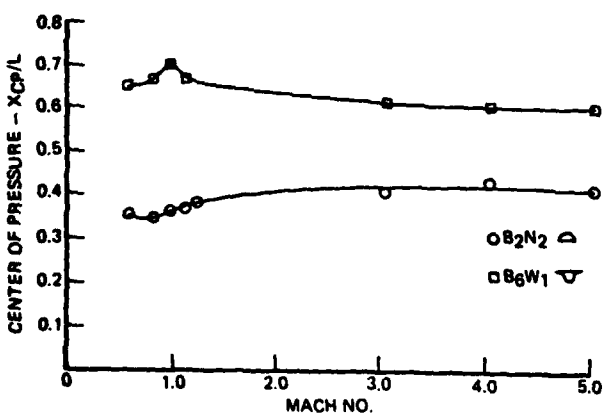

FIGURE 17 STABILITY CHARACTERISTICS

Transonic Characterisitcs

The increased transonic lift effectiveness of the wing is evident in the plot of lift curve slope versus Mach number in Fig. 18. These results (which were typical for all configurations) show a distinctly higher lift curve slope at transonic Mach number for wings or fins. Body alone configurations show relatively little change in lift curve slope with Mach number. The change in drag characteristics with Mach number is shown in Fig. 19. Wing and fin configurations exhibited strong transonic drag rises when compared to bodies.

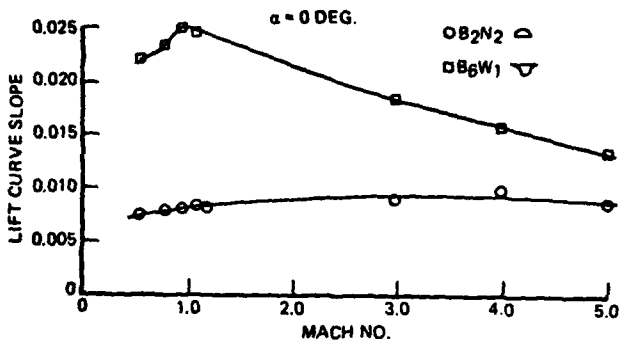

FIGURE 18 TRANSONIC LIFT CHARACTERISTICS

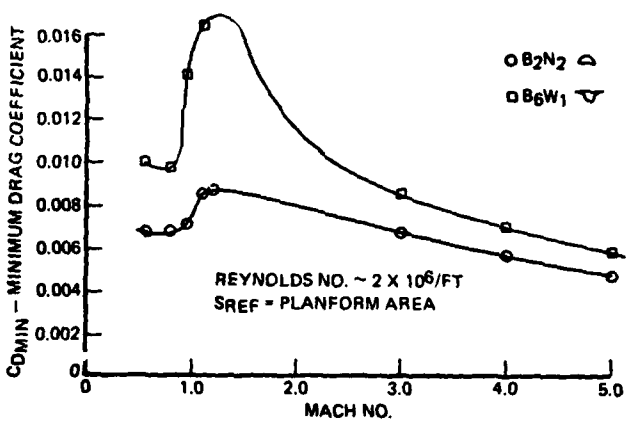

FIGURE 19 TRANSONIC MINIMUM DRAG

Configuration Summary

A summary of the aerodynamic potential of the real configurations to satisfy the benchmark cruise and maneuvering missions is shown in Fig. 20. The configuration exhibiting the highest lift-over-drag ratio for both missions was the B_3 N_8 lifting body. In addition, its nearly neutral stability characteristics (forward X_{CP}) during cruise gives it high potential to reduce trim drag. However B_2 N_2 F_2 and B_6 W_1 were also promising configurations and all three will be carried into Phase II of the Ref. 1 program. Constraints will be applied during this phase and further wind tunnel tests performed.

CONFIGURATION	CRUISE ALTITUDE, KFT	CRUISE MISSION			MANEUVERING MISSION (90 KFT)		
		α OPT, DEG.	(L/D) MAX.	$X_{CP/L}$ (α OPT)	α MAN., DEG.	(L/D) α MAN.	$X_{CP/L}$ MAN.
B_2N_2	82.4	5.5	5.4	0.41	20.4	2.4	0.49
$B_2N_2F_2$	86.9	5.0	5.7	0.54	17.3	2.8	0.54
B_3N_8	91.6	4.7	6.0	0.54	14.2	3.4	0.58
B_5W_1	96.0	4.5	5.3	0.61	14.5	3.0	0.68
B_6W_1	96.4	4.1	5.8	0.61	14.1	3.2	0.66

FIGURE 20 CONFIGURATION PERFORMANCE SUMMARY

Conclusions

The Phase I ACM unconstrained concepts were shown to exhibit high lift-over-drag ratios and good potential for satisfying cruise and maneuvering missions.

The Hypersonic Arbitrary Body Program was shown to be a valuable tool in configuration development.

The successful testing of a variety of shapes and plan forms provides an excellent data base both for future reconfiguring as well as prediction code calibration.

Bibliography

[1]Aerodynamic Configured Missile Development, Air Force Flight Dynamics Laboratory Contract F33615-77-C-3037 (AFFDL/FXG)

[2]Gentry, A. E., Smyth, D. N. and Oliver, W. R., The Mark IV Supersonic-Hypersonic Arbitrary-Body Program, Volume I Users Manual, Vol. II Program Formulation, Vol. III Program Listings, Technical Report AFFDL-TR-73-159.